

Vorticity generated by pure capillary waves

By SHAHRDAD G. SAJJADI

Institute for Nonlinear Science, University of California at San Diego, 9500 Gilman Drive,
La Jolla, CA 92093, USA

(Received 1 February 2000 and in revised form 12 July 2001)

Capillary waves, like other surface waves on water, generate a rectified, or time-averaged, vorticity field extending beyond the oscillatory (Stokes) layer at the surface. This vorticity field ω is particularly interesting in relation to the parasitic capillary waves found on the forward slopes of steep gravity waves. Longuet-Higgins (1992) suggested that the rectified vorticity from the parasitic capillaries might contribute significantly to the vorticity observed beneath the crest of the gravity wave. The basic calculations by Longuet-Higgins (1992) were only of the horizontally averaged values of ω . Here we extend his theory by calculating, for pure capillary waves, the space variation of ω , to second order in the steepness of the capillary waves. Thus, the vorticity, and hence velocity, fields are calculated in the oscillatory Stokes layer and just beyond it, to the second order. Good agreement is found both with numerical simulations and with experimental measurements.

1. Introduction

Recently there has been increased interest in the small-scale structures of wind waves, partly because of the importance of wavelengths of order 1 cm to the remote sensing of the sea surface but more basically because short waves are believed to affect the large-scale transfers of heat, gases and momentum between the ocean and the atmosphere.

The capillary waves formed on the forward face of relatively short gravity waves have proven to be a common phenomenon occurring at the surface of wind-driven bodies of water. Thus, the more accurate representation of such capillary waves furthers the understanding of air–sea fluxes, such as those of momentum, gas and mass. Indeed, the mass transfer coefficient at air–sea interaction remains the second most uncertain parameter in the greenhouse effect in climate modelling. Moreover, most widely accepted theories of wind-wave generation (Miles 1957; Phillips 1957) and their recent extensions (Miles 1996 for linear waves and Sajjadi, Wakefield & Croft 1997, Sajjadi 1998 for nonlinear waves) neglect the nonlinear effects of gravity–capillary waves. The recent measurements of wind-generated surface waves by Klinke (1996) indicate that very soon after the initial stages of wave generation the steepness of gravity waves reaches the threshold necessary for the appearance of capillaries which influence the dissipative and other dynamical properties of the surface waves.

Pure capillary waves are also important for variety of reasons:

(i) they provide a mechanism for extracting energy from the primary gravity wave through viscous energy dissipation at the much shorter capillary lengthscale;

Present address: CHL, John C. Stennis Space Center, Building 1103, Suite 103, Mississippi 39529, USA.

- (ii) they generate surface roughness at wavelengths which scatter electromagnetic radiation thereby improving the remote sensing of the ocean surface by microwaves;
- (iii) their presence or absence helps us in the study of sea slicks and sea surface chemistry;
- (iv) they provide a source of near-surface vorticity, as shown by Longuet-Higgins (1992).

Surprisingly little information is available on these waves, due to the analytical, numerical and experimental difficulties involved.

Longuet-Higgins (1992) was especially concerned with the near-surface vorticity produced by capillary waves. He calculated the oscillatory component of the vorticity to order ak , where a and k denote the amplitude and wavenumber of the capillary waves, and also the horizontally averaged vorticity (which diffuses to greater depths) to order $(ak)^2$.

The aim of this paper is to extend Longuet-Higgins' (1992) theory to take into account the complete distribution in space of the vorticity field, to second order in ak . Thus the vorticity and velocity fields will be calculated in the boundary layer, and just beyond it, to the second order. Also, the horizontal mean flow will be calculated, to the second order, as a function of the vertical coordinate or the coordinate normal to the local mean surface.

Our analytical results will be compared with a numerical simulation of parasitic capillary waves due to Mui & Dommermuth (1995) and with the experiments of Lin & Perlin (1998). It should be noted that the calculations of Mui & Dommermuth (1995) could only be performed with difficulty for gravity waves of length 5 cm or less. However, our theoretical results are valid for gravity wavelengths beyond this limit.

We emphasize that the ordering parameter chosen for the perturbation expansion in this work is the wave steepness ak for the ripple and not the wave steepness of the longer wave. Moreover, throughout this work we will assume $ak \ll 1$. The ripples, or 'parasitic capillary waves', are so short that they may be treated as pure capillary waves.

2. Second-order boundary-layer theory

We shall first recall the boundary-layer theory for viscous capillary waves, due to Longuet-Higgins (1992). The present theory is applicable to steeper waves of order a^2k^2 , where ak is the wave steepness.

The starting point is the equation for the vorticity ω , namely

$$\left(\nu \frac{\partial^2}{\partial n^2} - \bar{q} \frac{\partial}{\partial s} \right) \omega = q'_{sl} \frac{\partial \omega}{\partial s} - n \frac{\partial q'_{sl}}{\partial s} \frac{\partial \omega}{\partial n}, \quad (2.1)$$

where (s, n) denote coordinates tangential and normal to any streamline in a steady, two-dimensional flow, \bar{q} is the mean speed of a particle along the boundary, q'_{sl} represents the tangential component of the orbital velocity and ν is the kinematic viscosity.

The boundary conditions imposed on (2.1) are

$$\left. \begin{aligned} \omega &= -2\kappa(\bar{q} + q'_{sl}) & \text{when } n &= 0, \\ \nabla \omega &\rightarrow 0 & \text{as } n &\rightarrow \infty, \end{aligned} \right\} \quad (2.2)$$

where κ is the curvature of the streamline.

To solve (2.1), we seek a perturbation expansion in powers of an ordering parameter ε which we take to be the wave steepness ak . Thus we write

$$\omega = \varepsilon\omega_1 + \varepsilon^2\omega_2 + \dots, \tag{2.3}$$

$$q'_{s1} = \varepsilon q_{s11} + \varepsilon^2 q_{s12} + \dots, \tag{2.4}$$

$$\kappa = \varepsilon\kappa_1 + \varepsilon^2\kappa_2 + \dots, \tag{2.5}$$

Substituting (2.3)–(2.5) into (2.1) and (2.2) we obtain to $O(\varepsilon)$

$$\left(v \frac{\partial^2}{\partial n^2} - \bar{q} \frac{\partial}{\partial s} \right) \omega_1 = 0 \tag{2.6}$$

and

$$\left. \begin{aligned} \omega_1 &= -2\kappa_1 \bar{q} \quad \text{when } n = 0, \\ \frac{\partial \omega_1}{\partial n} &\rightarrow 0 \quad \text{as } n \rightarrow \infty. \end{aligned} \right\} \tag{2.7}$$

By expanding κ_1 as a Fourier series in s

$$\kappa_1 = \sum_{\ell=0}^{\infty} C_{\ell} e^{i\ell K s}, \quad K = 2\pi/s_{\max}, \tag{2.8}$$

Longuet-Higgins (1992) found the following solution for ω_1 †:

$$\omega_1 = -2\bar{q} \sum_{\ell=1}^{\infty} C_{\ell} e^{i\ell K s - \ell^{1/2} \alpha n}, \tag{2.9}$$

where

$$\alpha^2 = i\sigma/v, \quad \text{Re}(\alpha) > 0. \tag{2.10}$$

Here $\sigma = kc$ is the radian frequency and c is the phase speed.

At second order, $O(\varepsilon^2)$, Longuet-Higgins (1992) used only the averaged form of equation (2.1), but here we shall require the full equation for ω_2 , which is

$$\left(v \frac{\partial^2}{\partial n^2} - \bar{q} \frac{\partial}{\partial s} \right) \omega_2 = q_{s11} \frac{\partial \omega_1}{\partial s} - n \frac{\partial q_{s11}}{\partial s} \frac{\partial \omega_1}{\partial n}, \tag{2.11}$$

which has to be solved subject to the following boundary conditions:

$$\left. \begin{aligned} \omega_2 &= -2(\kappa_1 q_{s11} + \kappa_2 \bar{q}) \quad \text{when } n = 0, \\ \frac{\partial \omega_2}{\partial n} &\rightarrow 0 \quad \text{as } n \rightarrow \infty. \end{aligned} \right\} \tag{2.12}$$

Taking Laplace transform of (2.11) we obtain

$$\frac{d\hat{\omega}_2}{ds} - \beta \xi^2 \hat{\omega}_2 = \hat{f}(s, \xi) - h(s, n = 0), \tag{2.13}$$

where $\hat{\omega}_2(s, \xi)$ and $\hat{f}(s, \xi)$ represent the Laplace transforms of ω_2 and the right-hand side of equation (2.12) with respect to n , respectively. In equation (2.13) $\beta = v/\bar{q}$ and

$$h(s, n = 0) = \beta \left(\frac{\partial \omega_2}{\partial n} + \xi \omega_2 \right)_{n=0}. \tag{2.14}$$

† Note that equation (2.9) is analogous to equation (3.11) of Fedorov & Melville (1998) for nonlinear gravity-capillary waves.

In order to solve equation (2.13) uniquely we must *a priori* determine the expression (2.14) and the initial condition $\hat{\omega}_2(0)$, correct to second order.

3. Second order vorticity at a free surface

Longuet-Higgins (1953, 1992) showed that in any steady flow in which the tangential stress vanishes, the vorticity at the surface is given by

$$\omega_s = -2\kappa q. \quad (3.1)$$

In what follows we shall use (3.1) to determine $\omega_2(s, 0)$, $(\partial\omega_2/\partial n)_{n=0}$ and $\hat{\omega}_2(0)$.

Choosing units of length and time such that the phase speed c and wavenumber k become 1 and 2 respectively, Crapper's (1957) solution for pure capillary waves becomes

$$z = w - \tan w, \quad (3.2)$$

where $z = x + iy$ and $w = \varphi + i\psi$, in the reference frame moving to the left with velocity $-c$. Note that any streamline $\psi = \psi_0$ is a line of constant pressure and may be chosen as the free surface. Thus a family of waves specified by the parameter

$$A = e^{-2\psi_0} \quad (3.3)$$

may be obtained in the range $0 < A < 0.4547$, that is $\infty > \psi_0 > 0.3941$ (Longuet-Higgins 1997). The maximum angle of slope of the free surface is related to A by

$$\alpha_{\max} = 4 \tan^{-1} A. \quad (3.4)$$

Note that in the linearized theory $\alpha_{\max} \approx ak$.

From equation (3.2) we see that

$$\frac{dz}{dw} = 1 - \sec^2 w = -\tan^2 w \quad (3.5)$$

and thus

$$q = \left| \frac{dw}{dz} \right| = \cot w \cot w^*, \quad (3.6)$$

where the superscript $*$ denotes the complex conjugate. Following Longuet-Higgins (1988) the surface curvature κ may be expressed as

$$\kappa = \frac{\cos 2\varphi \sinh 2\psi_0}{\sin^2 w \sin^2 w^*}. \quad (3.7)$$

Hence by writing $\zeta = e^{2i\varphi}$ we obtain

$$\begin{aligned} \kappa q &= 4A(1 - A^2) \frac{\zeta(\zeta^2 + 1)(A\zeta + 1)(A + \zeta)}{(A\zeta - 1)^3 n(A - \zeta)^3} \\ &= 4A(1 - A^2)F(\theta), \end{aligned} \quad (3.8)$$

where for convenience we have set $\theta = 2\varphi$.

We now express $F(\theta)$ as a Fourier series

$$F(\theta) = \operatorname{Re} \sum_{n=0}^{\infty} a_n e^{-in\theta}, \quad (3.9)$$

where the Fourier coefficients a_n are given by

$$a_n = \frac{1}{\pi} \int_0^{2\pi} F(\theta) e^{in\theta} d\theta. \tag{3.10}$$

Substituting $\zeta = e^{i\theta}$ equation (3.10) becomes

$$a_n = \frac{1}{\pi i} \oint_{|\zeta|=1} \frac{(\zeta^2 + 1)(A + \zeta)(A\zeta + 1)}{(A - \zeta)^3 (A\zeta - 1)^3} \zeta^n d\zeta. \tag{3.11}$$

Since $|A| < 1$ the integrand has just one pole within the unit circle, namely at $\zeta = A$. Upon taking $2\pi i$ times the residue at this point (found by letting $\zeta = A + \varepsilon$ in the integrand, expanding in powers of ε , and taking $2\pi i$ times the coefficient of ε^{-1}) we obtain

$$a_1 = 2[1 + 25A^2 + O(A^3)], \quad a_2 = 2[4A + O(A^3)], \quad a_3 = 2[9A^2 + O(A^3)], \tag{3.12}$$

etc. Hence

$$F(\varphi) = 2[(1 + 25A^2) \cos 2\varphi + 4A \cos 4\varphi + 9A^2 \cos 8\varphi] + O(A^3). \tag{3.13}$$

We shall now use (3.13) to construct a Fourier series representation of κq in terms of s , namely the tangential coordinate to the streamline. Using (3.6) it may be shown that

$$q = \frac{(1 + A\zeta)(1 + A\zeta^{-1})}{(1 - A\zeta)(1 - A\zeta^{-1})} \tag{3.14}$$

and since $d\varphi/ds = q$, upon expressing φ in terms of ζ we may write

$$s = \frac{1}{2i} \oint_{|\zeta|=1} \frac{(1 - A\zeta)(1 - A\zeta^{-1})}{(1 + A\zeta)(1 + A\zeta^{-1})} \frac{d\zeta}{\zeta}. \tag{3.15}$$

The integrand has simple poles at the origin and at $\zeta = A$ within the unit circle. Upon taking $2\pi i$ times the sum of residue we obtain

$$s = \frac{\pi(1 + 3A^2)}{1 - A^2}. \tag{3.16}$$

We next need to express s in the half-range Fourier sine series

$$s = D_0\varphi + \sum_{k=0}^{\infty} b_k \sin k\varphi, \tag{3.17}$$

where $D_0 = 1 + O(A^2)$ and the Fourier coefficients b_k are given by

$$b_k = \frac{2}{\pi} \int_0^\pi (s - \varphi) \sin k\varphi d\varphi. \tag{3.18}$$

Performing the integration and substituting the coefficients b_k into (3.17) we obtain the following Fourier representation of s in terms of φ :

$$s = D_0\varphi + 4 \left(\frac{1 + 3A^2}{1 - A^2} \right) \sum_{k=0}^{\infty} \frac{\sin[(2k + 1)\varphi]}{2k + 1} + 2D_0 \sum_{k=0}^{\infty} \frac{\cos(2k + 1)\pi}{(2k + 1)^2} \sin[(2k + 1)\varphi] \tag{3.19}$$

Finally we express κq in the following form:

$$\kappa q = \sum_{m=0}^{\infty} c_m e^{ims}, \quad (3.20)$$

where

$$c_m = \frac{2}{\pi} \int_0^{\pi} F(\varphi) e^{-ims} ds. \quad (3.21)$$

Now substituting the expression for s from equation (3.19), after expanding the fraction $(1 + 3A^2)(1 - A^2)^{-1}$ as a binomial series in A^2 , together with the expression for $F(\varphi)$ from (3.13) into (3.21), performing the integration and substituting the result for c_m into (3.20) we obtain

$$\kappa q = \frac{2D_0}{\pi} \sum_{m=0}^{\infty} m(\alpha_m + \beta_m A + \gamma_m A^2) e^{im\pi s} + O(A^3), \quad (3.22)$$

where

$$\begin{aligned} \alpha_m &= (10.12m\pi + 19.63i) + (1.65m\pi - 7.99i)D_0 - 2.73m\pi D_0^2, \\ \beta_m &= (40.92m\pi + 76.18i) + (20.95m\pi - 14.05i)D_0 - 7.28m\pi D_0^2, \\ \gamma_m &= (294.34m\pi + 592.2i) + (88.87m\pi - 204.39i)D_0 - 76.62m\pi D_0^2. \end{aligned}$$

Hence the vorticity at the surface to the second order is

$$\omega_{2s} = -\frac{4D_0}{\pi} \sum_{m=0}^{\infty} m(\alpha_m + \beta_m A + \gamma_m A^2) e^{im\pi s} + O(A^3). \quad (3.23)$$

4. Second-order vorticity in the boundary layer

Before solving equation (2.13), in the light of the expression for the vorticity at the free surface and the solution for ω_1 , equation (2.9), we make the assumption that

$$\omega_2(0, n) = -\frac{4D_0}{\pi} \sum_{\ell=0}^{\infty} \ell \gamma_{\ell} \exp(-\ell^{1/2} \alpha n) \quad (4.1)$$

correct to second order. This assumption can be justified due to periodicity. The Laplace transform of equation (4.1), namely

$$\hat{\omega}_2(0) = -\frac{4D_0}{\pi} \sum_{\ell=0}^{\infty} \frac{\ell \gamma_{\ell}}{\ell^{1/2} \alpha + \xi}, \quad (4.2)$$

will serve as an initial condition for the differential equation (2.13). Note that (4.1) also implies that $(\partial \omega_2 / \partial n)_{n=0} = 0$.

Expressing q_{s11} as a Fourier series in s

$$q_{s11} = \sum_{\ell=1}^{\infty} B_{\ell} e^{iK_{\ell} s}, \quad (4.3)$$

substituting it together with the solution for ω_1 from (2.9) in the expression for $f(s, n)$ and taking its Laplace transform we obtain

$$\hat{f}(s, \xi) = 2iK \sum_{\ell=1}^{\infty} \sum_{m=1}^{\infty} B_{\ell} C_m e^{i(\ell+m)Ks} \left\{ \frac{\alpha \ell m^{1/2}}{(\alpha m^{1/2} + \xi)^2} + \frac{m}{\alpha m^{1/2} + \xi} \right\}, \quad (4.4)$$

Now substituting the expression for $\omega_{2s} \equiv \omega_2(s, 0)$ from (3.23) into (2.14) and subtracting the result from (4.4), equation (2.13) becomes

$$\frac{d\hat{\omega}_2}{ds} - \beta\xi^2\hat{\omega}_2 = 2Ki \sum_{\ell=1}^{\infty} \sum_{m=1}^{\infty} B_{\ell}C_m e^{i(\ell+m)Ks} \left\{ \frac{\alpha\ell m^{1/2}}{(\alpha m^{1/2} + \xi)^2} + \frac{m}{\alpha m^{1/2} + \xi} \right\} + \frac{4D_0}{\pi} \beta\xi \sum_{\ell=0}^{\infty} \ell\gamma_{\ell} e^{i\ell\pi s}. \quad (4.5)$$

Solving equation (4.5) using integrating factor we obtain

$$\hat{\omega}_2(s) = 2 \sum_{\ell=1}^{\infty} \sum_{m=1}^{\infty} B_{\ell}C_m \left\{ \frac{e^{i(\ell+m)Ks} - 1}{\ell + m} \right\} \left\{ \frac{\alpha\ell m^{1/2}}{(\alpha m^{1/2} + \xi)^2} + \frac{m}{\alpha m^{1/2} + \xi} \right\} - \frac{4iD_0}{\pi^2} \sum_{\ell=0}^{\infty} \left\{ \beta\xi(e^{i\ell\pi s} - 1) - \frac{i\pi\ell\gamma_{\ell}}{\ell^{1/2}\alpha + \xi} \right\}. \quad (4.6)$$

Hence $\omega_2(s, n)$ can be obtained using the complex inversion formula

$$\omega_2 = \frac{1}{\pi i} \sum_{\ell=1}^{\infty} \sum_{m=1}^{\infty} B_{\ell}C_m \left\{ \frac{e^{i(\ell+m)Ks} - 1}{\ell + m} \right\} \int_{\varpi-i\infty}^{\varpi+i\infty} \left\{ \frac{\alpha\ell m^{1/2}}{(\alpha m^{1/2} + \xi)^2} + \frac{m}{\alpha m^{1/2} + \xi} \right\} \times e^{i\xi n} d\xi - \frac{2D_0}{\pi^3} \sum_{\ell=0}^{\infty} \int_{\varpi-i\infty}^{\varpi+i\infty} \left\{ \beta\xi(e^{i\ell\pi s} - 1) - \frac{i\pi\ell\gamma_{\ell}}{\ell^{1/2}\alpha + \xi} \right\} e^{i\xi n} d\xi. \quad (4.7)$$

The first and the third integrals in (4.7) are zero. However, the second and the fourth integrals have a simple pole at $\xi = -\alpha m^{1/2}$ and $\xi = -\alpha \ell^{1/2}$, respectively. Calculating the residue at these poles we obtain the following solution for the second-order vorticity:

$$\omega_2(s, n) = \frac{1}{\pi i} \sum_{\ell=1}^{\infty} \sum_{m=1}^{\infty} m B_{\ell}C_m \left\{ \frac{e^{i(\ell+m)Ks} - 1}{\ell + m} \right\} e^{-i\alpha m^{1/2}n} - \frac{4D_0}{\pi} \sum_{\ell=0}^{\infty} \ell\gamma_{\ell} e^{-i\alpha \ell^{1/2}n}. \quad (4.8)$$

5. The total vorticity

Following Longuet-Higgins (1992) the total vorticity ω is decomposed as

$$\omega(s, n, t) = \bar{\omega}(n, t) + \tilde{\omega}(s, n), \quad (5.1)$$

where $\bar{\omega}$ and $\tilde{\omega}$ denote the mean and the periodic components of the vorticity, respectively, and

$$\tilde{\omega}(s, n) = \varepsilon\omega_1(s, n) + \varepsilon^2\omega_2(s, n) + \dots$$

Longuet-Higgins (1992) argued that unlike the periodic component, the mean vorticity diffuses into the interior of the fluid on a longer time scale than the wave period, according to the diffusion equation

$$\frac{\partial \bar{\omega}}{\partial t} = \nu \frac{\partial^2 \bar{\omega}}{\partial n^2}. \quad (5.2)$$

Note that when n becomes comparable with k^{-1} , we may replace n with z , where z is the mean depth of a particle below the mean surface level. Now if the motion is



FIGURE 1. Part of the subsurface vorticity field computed numerically by Mui & Dommermuth (1995; their figure 8) for a 5 cm gravity wave. The horizontal distance shown is 2.98 cm. The free surface is plotted with the same vertical and horizontal scale, so that the surface slope is represented correctly. However for the flow beneath the surface, the vertical scale has been dilated; the total vertical extent is only 1 mm.

started at $t = 0$, on these time and length scales, the solution of (5.2) is

$$\bar{\omega} = \frac{2\bar{\omega}_{\infty}}{\sqrt{\pi}} \int_Z^{\infty} e^{-\lambda^2} d\lambda, \quad (5.3)$$

where $Z = z/2\sqrt{vt}$ and $\bar{\omega}_{\infty} = -2(ak)^2\sigma$.

The horizontal velocity \bar{u} associated with the mean vorticity is given by

$$\bar{u} = \int_z^{\infty} \bar{\omega}(z, t) dz. \quad (5.4)$$

Substituting (5.3) into (5.4) we see that

$$\bar{u} = 4\sqrt{\frac{vt}{\pi}} \bar{\omega}_{\infty} \left[\frac{e^{-Z^2}}{2} - Z \int_Z^{\infty} e^{-\lambda^2} d\lambda \right]. \quad (5.5)$$

At the mean surface level $z = 0$ equation (5.5) reduces to

$$\bar{u}_0 = -2\sqrt{\frac{vt}{\pi}} \bar{\omega}_{\infty} \quad (5.6)$$

which may be alternatively cast in the form

$$\bar{u}_0 = -2N^{1/2}\delta\bar{\omega}_{\infty}, \quad (5.7)$$

where $N = \sigma t/2\pi$ is the number of wave cycles after starting the motion and $\delta = \sqrt{2v/\sigma}$ is the boundary-layer thickness.

ψ_0	λ (cm)	A	ak	α_{\max}	$2\kappa_1\bar{q}$	ω_{\min} (s ⁻¹)	ω_{\max} (s ⁻¹)	D_N
1.0138	0.446	0.1317	0.5266	0.5236	-479	-483	92	0.68
1.0670	0.402	0.1184	0.4734	0.4712	-503	-508	119.16	0.62
1.2710	0.357	7.8701×10^{-2}	0.3148	0.3142	-400	-404	85.7	0.65
1.4342	0.335	5.6784×10^{-2}	0.2271	0.2269	-317	-319.98	80	0.6

TABLE 1. Summary of theoretical results

6. Results

We shall now compare our theoretical results with the numerical calculation by Mui & Dommermuth (1995) of the vorticity and velocity fields in a gravity wave of length 5 cm. Starting with a pure gravity wave of steepness 0.2827 they first solved the inviscid equations and boundary conditions, and found as expected that parasitic capillary waves (ripples) quickly developed on the forward face. At time $t = 4.5$ they switched to the full Navier–Stokes equations. The computed vorticity field at time $t = 4.8416$, when the flow appeared almost steady, is shown in their figure 8, a part of which is shown enlarged in figure 1. The free surface is drawn to scale but for the subsurface flow the vertical scale is enlarged; the vertical distance shown corresponds to only 1 mm in reality. The gravity wave travels from right to left. There are four distinct wave troughs in the train of ripples ahead of the main crest. The crest-to-crest wavelengths λ and the mean steepnesses ak of these ripples are shown in table 1. Note that the minimum and the maximum values of vorticities, quoted in table 1, refer to the total vorticity, i.e. $\omega = \bar{\omega} + \varepsilon\omega_1 + \varepsilon^2\omega_2$.

Since the ripples are essentially stationary relative to the crest of the gravity wave, they can be regarded as travelling to the right, in a frame moving with the phase speed of the gravity wave. We see that just ahead of each wave trough there is a plume of positive vorticity extending downwards at an angle for half a wavelength or more. Likewise, in the crest of each ripple the vorticity is negative.

For comparison we show in figures 2(a) to 2(d) our theoretical calculations of the vorticity field for four capillary waves having the same values of λ and ak as in table 1. Qualitatively the contours of vorticity are very similar in each case, with plumes of positive vorticity extending downwards beneath the wave troughs. Quantitatively, the minimum vorticity according to our theory is -483 s^{-1} compared to the value -224 s^{-1} in the numerical calculation of Mui & Dommermuth. The maximum vorticity according to our theory is 92 s^{-1} compared to Mui & Dommermuth's 210 s^{-1} . Note that their values of vorticity are scaled with the factor $\sqrt{g/L}$, where g is the acceleration due to gravity, and $L = 5 \text{ cm}$ is the total length of the ripples.

We can also make a comparison between our theory and the experimental results of Lin & Perlin (1998), who used particle image velocimetry to measure the vorticity generated by ripples from a gravity–capillary wave of length 5 cm and steepness 0.16. In figure 3 we have sketched the contours of vorticity from figure 5(a) of the review paper by Perlin & Schultz (2000). Judging from the colour scheme of their plot we estimate their maximum and minimum vorticities to be about 140 s^{-1} and -210 s^{-1} respectively. For comparison we show in figure 4 our theoretical calculation of the vorticity contours beneath a pure capillary wave of length 5 mm and steepness $ak = 0.1$ (for this calculation $\psi_0 = 1.84$). The calculated maximum and minimum vorticities are 21.5 s^{-1} and -81 s^{-1} respectively, in fair agreement with the measured values.

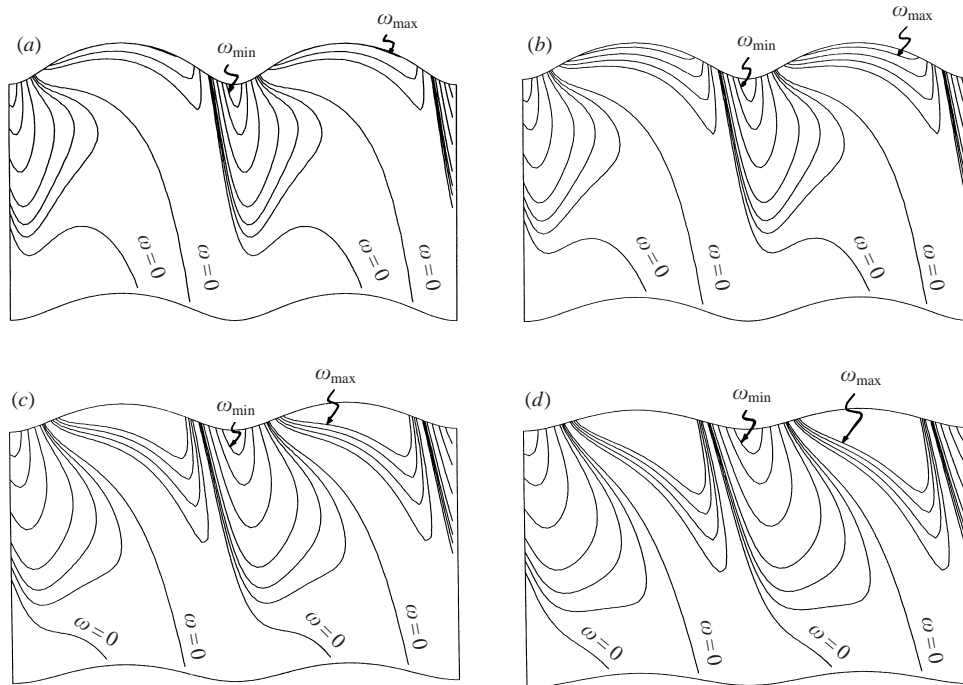


FIGURE 2. The total vorticity ($\omega = \bar{\omega} + \varepsilon\omega_1 + \varepsilon^2\omega_2$) contours at $t = 4.84$ s for a wave of (a) length $\lambda = 0.446$ cm and steepness $ak = 0.5266$, (b) $\lambda = 0.402$ cm and $ak = 0.4734$, (c) $\lambda = 0.357$ cm and $ak = 0.3148$, (d) $\lambda = 0.335$ cm and $ak = 0.2271$. The wave is travelling from left to right. The vertical coordinate is enlarged as in figure 1; the total depth shown is 0.5 mm.

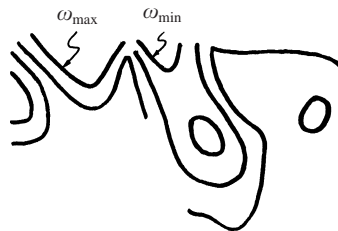


FIGURE 3. The vorticity distribution determined by Lin & Perlin (1998) (re-traced from part of figure 5(a) in Perlin & Schultz 2000).

In table 1 we also have also compared our numerical calculations with the first-order vorticity, given by (2.7). To the first order, we assume the surface profile is given by $y = a \cos kx$. Now taking $\kappa_1 = d^2y/dx^2$, approximating \bar{q} with $c = \sigma/k$ and setting $kx = \pi$ we obtain

$$\omega_{\min} = 2\kappa_1\bar{q} = -2ak^2c. \tag{6.1}$$

As can be seen from table 1 the present numerical calculations of the minimum vorticity agree well with those calculated by (6.1). Also tabulated in table 1 is the measure of the degree of nonlinearity D_N given by

$$D_N = \frac{|\omega_{\min}| - |\omega_{\max}|}{|\omega_{\min}| + |\omega_{\max}|}.$$

From their figure 1 we estimate D_N in the calculations of Mui & Dommermuth to

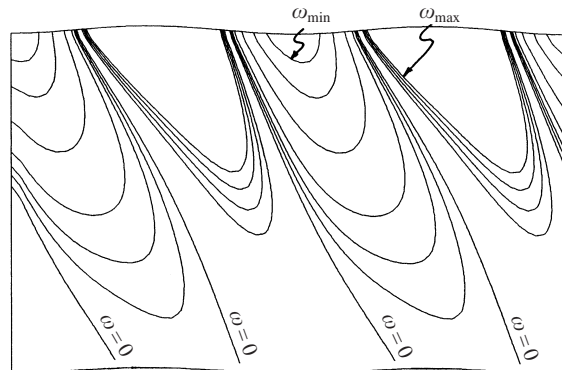


FIGURE 4. The caption is the same as figure 2 except $\lambda = 0.5$ cm and $ak = 0.1$.

be about 0.72. From our present calculations we observe that D_N lies in the range $0.58 \leq D_N \leq 0.68$, again in fair agreement with them.

Lastly we note that Lin & Rockwell (1995) have used particle image velocimetry to measure the vorticity field in waves forced by a subsurface aerofoil. At certain Froude numbers (particularly $Fr \approx 0.43$) they observe short waves of length 2 to 5 cm wavelength riding ahead of the gravity-wave crest. These are too long to be pure capillary ripples, but may be 'vortex waves' (see Longuet-Higgins 1994). Figure 4 of Lin & Rockwell (1995) shows that these 'Type 2' waves have regions of strong vorticity beneath the wave troughs but the distance of the vortices below the surface is much greater than in the 'Type 1' waves treated in the present paper.

7. Conclusions and discussion

We have extended the Longuet-Higgins (1992) averaged theory by calculating, for pure capillary waves, the space variation of the vorticity, to second order in the steepness of the capillary waves. Thus, the vorticity and velocity fields are calculated in the oscillatory boundary layer, and just beyond it, to the second order. Also, the horizontal mean flow and the vertical distribution of flow are calculated as a function of horizontal and vertical coordinates.

We have shown that regions of high vorticity are located near the troughs of the capillary waves where the vorticity induces strong surface currents. The theoretical results presented here agree very well, both qualitatively and quantitatively, with the experimental data of Lin & Perlin (1998) for the ripples on a 5 cm gravity wave. Our results are also in close agreement with the numerical simulations of Mui & Dommermuth (1995). However, it should be noted that the Mui & Dommermuth (1995) calculations could only be performed with difficulty for gravity waves of length not exceeding 5 cm. Their calculation did not or perhaps could not show any flow separation at the leading edge of the train of ripples, and hence the ripples did not contribute to the vorticity in the crest of the gravity wave. However, for longer gravity waves, such as are shown by Ebuchi, Kawamura & Toba (1987), the ripples may be steeper and flow separation may occur. Note that for longer gravity waves the ripples are shorter, and our calculations may still apply.

I would like to thank Professor Michael Longuet-Higgins for many fruitful discussions during the course of this research and his invitation for me to stay at the Institute for Nonlinear Science, University of California at San Diego to carry out

this research. Also my thanks go to the referees for their valuable suggestions. This work is supported in parts by EPSRC under the grant number GR/M72036. This paper is dedicated to the memory of my father, Shamseddin G. Sajjadi, 1920–2001.

REFERENCES

- COX, C. S. 1958 Measurements of slopes of high-frequency wind waves. *J. Mar. Res.* **16**, 199.
- CRAPPER, G. D. 1957 An exact solution for progressive capillary waves of arbitrary amplitude. *J. Fluid Mech.* **2**, 532.
- EBUCHI, N., KAWAMURA, H. & TOBA, Y. 1987 Fine structure of laboratory wind–wave surfaces studied using an optical method. *Boundary-Layer Met.* **39**, 133.
- FEDOROV, A. V. & MELVILLE, W. K. 1998 Nonlinear gravity–capillary waves with forcing and dissipation. *J. Fluid Mech.* **354**, 1.
- KLINKE, J. 1996 Optical measurements of small-scale wind-generated water surface waves in the laboratory and the field. PhD thesis. University of Heidelberg, Germany.
- LIN, H. J. & PERLIN, M. 1998 The velocity and vorticity fields beneath gravity–capillary waves exhibiting parasitic ripples. *Exs. Fluids* **24**, 431.
- LIN, J. C. & ROCKWELL, D. 1995 Evolution of a quasi-steady breaking wave. *J. Fluid Mech.* **302**, 29.
- LONGUET-HIGGINS, M. S. 1953 Mass transport in water waves. *Phil. Trans. R. Soc. Lond. A* **245**, 535.
- LONGUET-HIGGINS, M. S. 1960 Mass transport in the boundary layer at a free oscillatory surface. *J. Fluid Mech.* **8**, 293.
- LONGUET-HIGGINS, M. S. 1988 Limiting forms for capillary–gravity waves. *J. Fluid Mech.* **194**, 351.
- LONGUET-HIGGINS, M. S. 1992 Capillary rollers and bores. *J. Fluid Mech.* **240**, 659.
- LONGUET-HIGGINS, M. S. 1994 Shear instability in spilling breakers. *Proc. R. Soc. Lond. A* **446**, 399.
- LONGUET-HIGGINS, M. S. 1997 Viscous dissipation in steep capillary–gravity waves. *J. Fluid Mech.* **344**, 271.
- MILES, J. W. 1957 On the generation of surface waves by shear flows. *J. Fluid Mech.* **3**, 185.
- MILES, J. W. 1996 Surface wave generation: a viscoelastic model. *J. Fluid Mech.* **322**, 131.
- MUI, R. C. Y. & DOMMERMUTH, D. G. 1995 The vortical structure of parasitic capillary waves. *Trans. ASME: J. Fluids Engng* **117**, 355.
- PERLIN, M. & SCHULTZ, W. W. 2000 Capillary effects on surface waves. *Annu. Rev. Fluid Mech.* **32**, 241.
- PHILLIPS, O. M. 1957 On the generation of waves by turbulent wind. *J. Fluid Mech.* **2**, 417.
- SAJJADI, S. G. 1998 On the growth of a fully nonlinear Stokes wave by turbulent shear flow. Part 2: rapid distortion theory. *Math. Engng Ind.* **6**, 247.
- SAJJADI, S. G., WAKEFIELD, J. & CROFT, A. J. 1997 On the growth of a fully nonlinear Stokes wave by turbulent shear flow. Part 1: eddy-viscosity model. *Math. Engng Ind.* **6**, 185.